Diagnostic of welded structures using laser interferometry methods

L. Lobanov V. Pivtorak V. Savitsky*

Trzebnica, 3–6 th September 2013

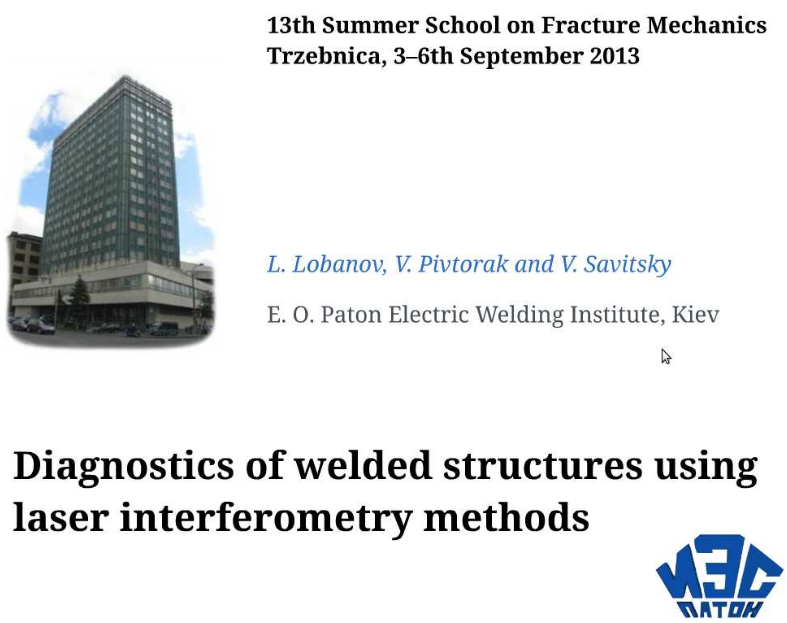

*Paton Electric Welding Institute, Kiev

laser interferometry

Holographic interferometry

Holographic interferometry

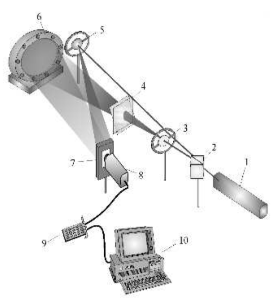

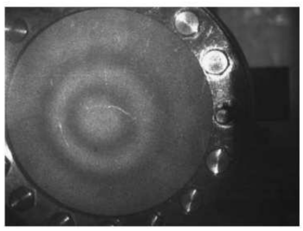

I = intensity + fringe contrast * cos(phase)

phase = (2π/λ)(Sensitivity vector . Deformation)

Holographic setup

1 - laser; 2 - beam splitter; 3, 5 - lenses, 6 - object; 7 - recording media; 8- CCD-camera; 9,10 - framegrabber and computer

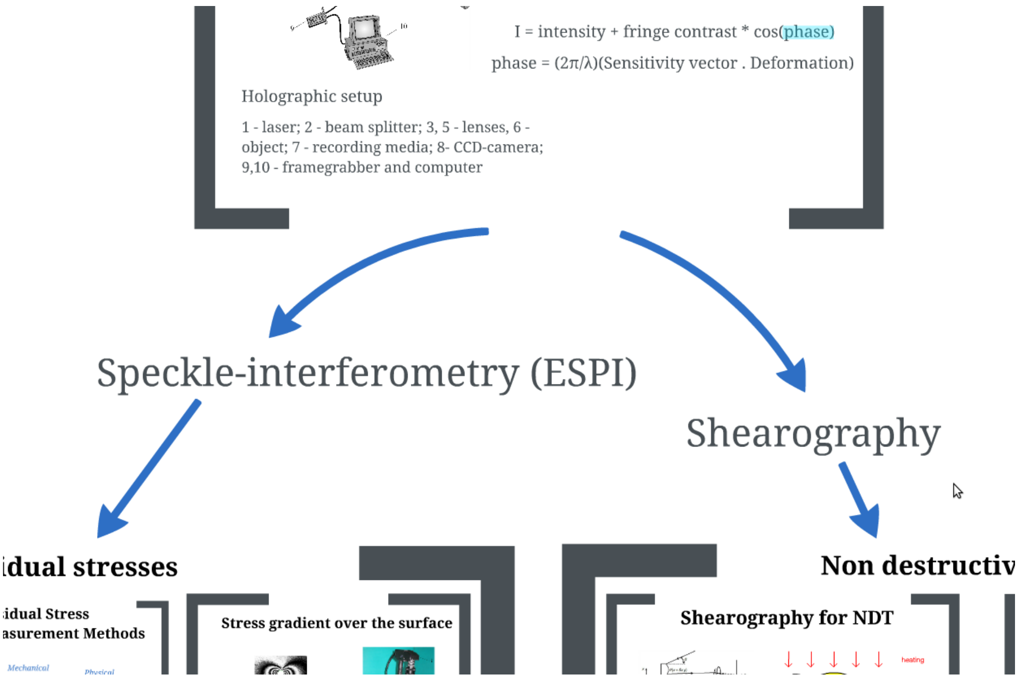
I = intensity + fringe contrast * cos(phase)
phase = (2π/λ)(Sensitivity vector . Deformation)
Holographic setup
1 - laser; 2 - beam splitter; 3, 5 - lenses, 6 - object; 7 - recording media; 8- CCD-camera; 9,10 - framegrabber and computer
Speckle-interferometry (ESPI)
Shearography
Stress gradient over the surface
Shearography for NDT
heating

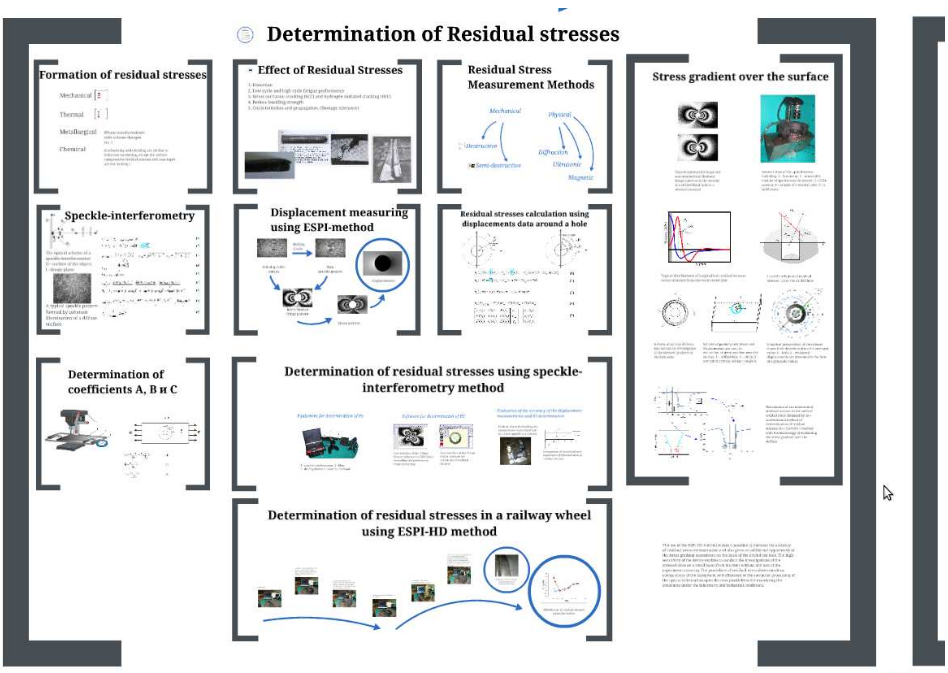
Determination of Residual stresses
Formation of residual stresses
Mechanical
Thermal
Metallurgical
Chemical
Effect of Residual Stresses
Residual Stress Measurement Methods
Mechanical
Physical
Stress gradient over the surface
Speckle-interferometry
Displacement measuring using ESPI-method
Residual stresses calculation using displacements data around a hole
Determination of coefficients A, B и C
Determination of residual stresses using speckle-interferometry method
Determination of residual stresses in a railway wheel using ESPI-HD method

What is Residual Stresses?

"the stress resident inside a component or structure after all applied forces have been removed"

Residual stress cannot be detected or evaluated by conventional surface measurement techniques, since the strain sensor (strain gage, photoelastic coating, etc.) can only respond to strain changes that occur after the sensor is installed

Formation of residual stresses

Mechanical 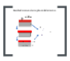

Thermal 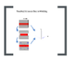

Metallurgical (Phase transformations with volume changes etc.)

Chemical (Carburizing and nitriding are similar to induction hardening, except the surface compressive residual stresses and case depth are not as deep.)

Mechanical

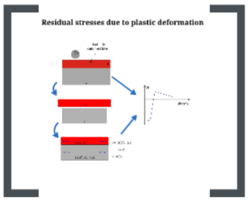

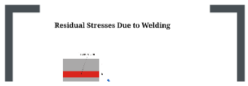

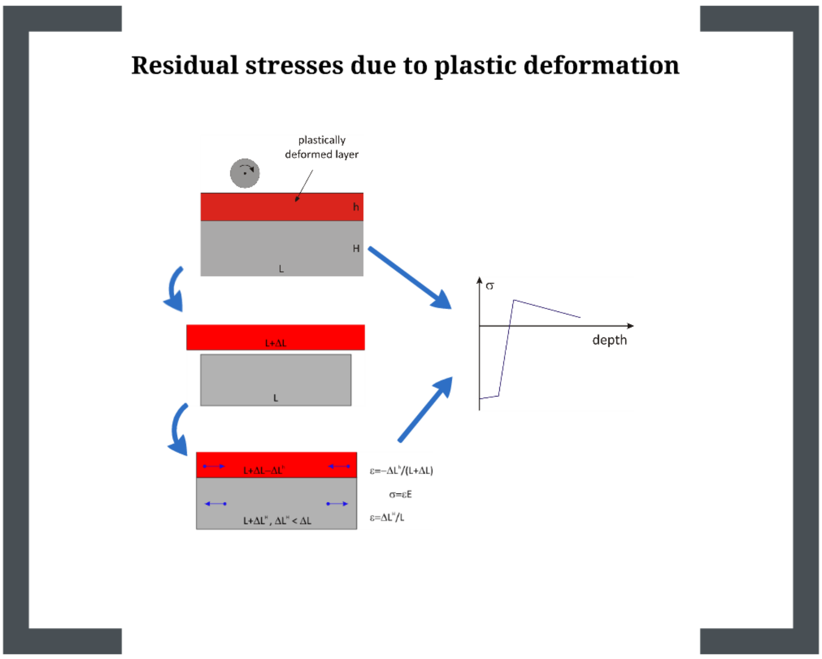
Residual stresses due to plastic deformation
plastically deformed layer
h
H
L
L+ΔL
L
L+ΔL−ΔL^h
L+ΔL^H , ΔL^H < ΔL
ε=−ΔL^h/(L+ΔL)
σ=εE
ε=ΔL^H/L
σ
depth

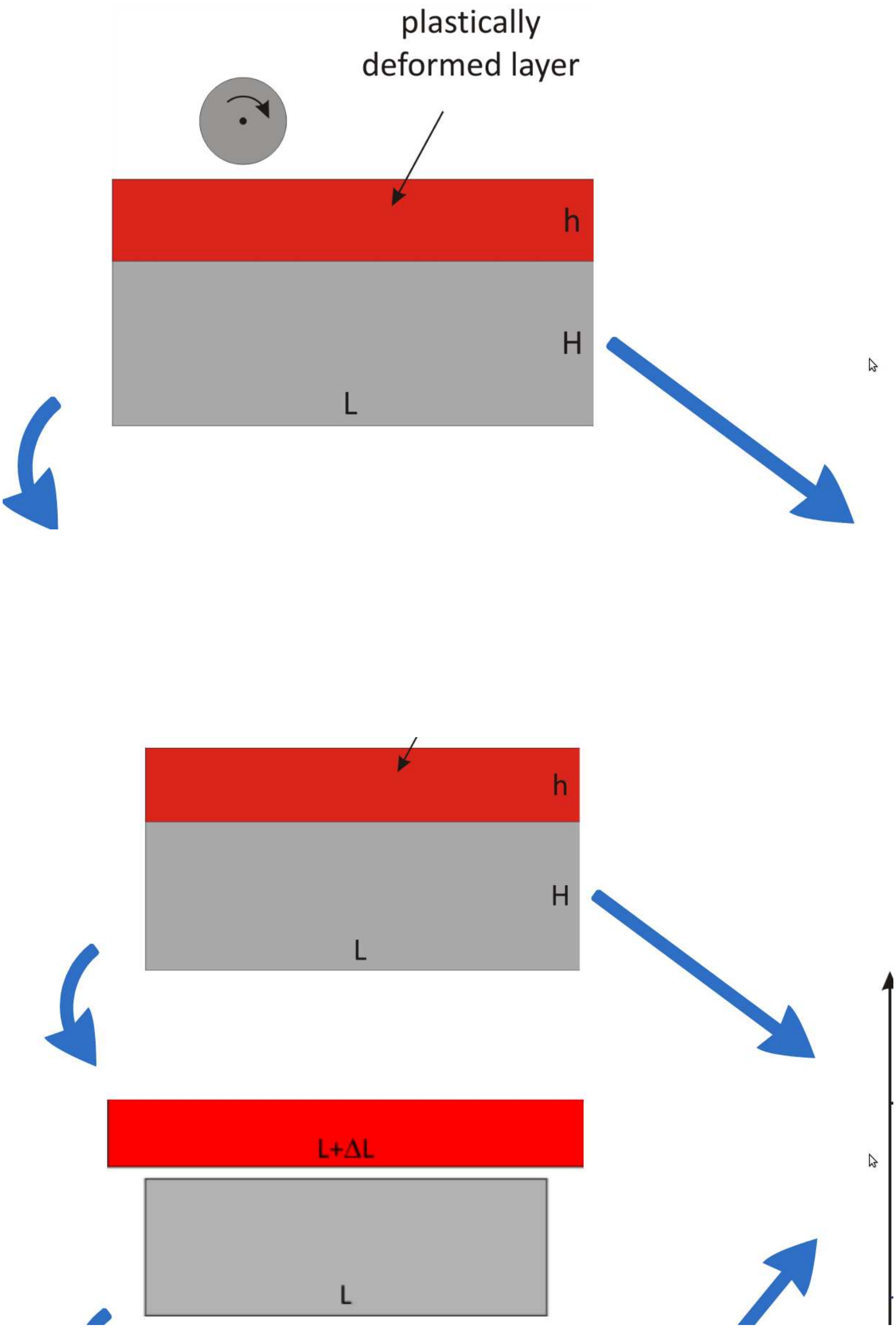
plastically
deformed layer
h
H
L
h
H
L
L+ΔL
L

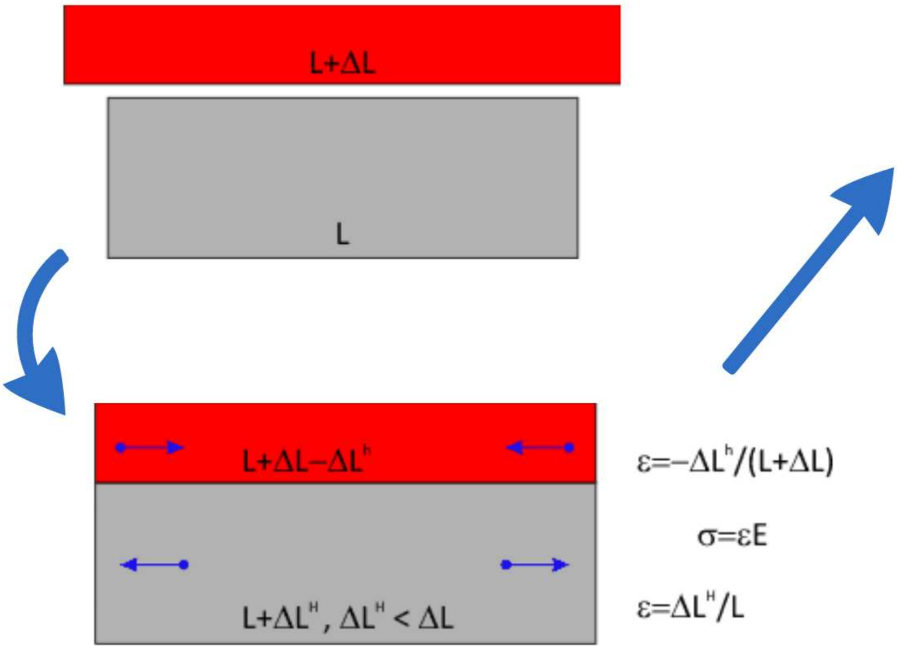
L+ΔL
L
L+ΔL−ΔL^h
L+ΔL^H, ΔL^H < ΔL
ε=−ΔL^h/(L+ΔL)
σ=εE
ε=ΔL^H/L

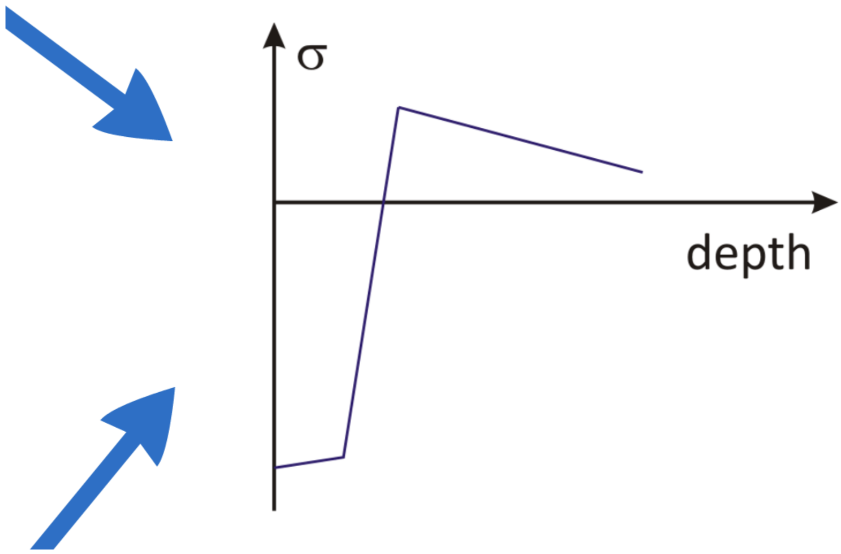
σ
depth

Residual stresses due to plastic deformation

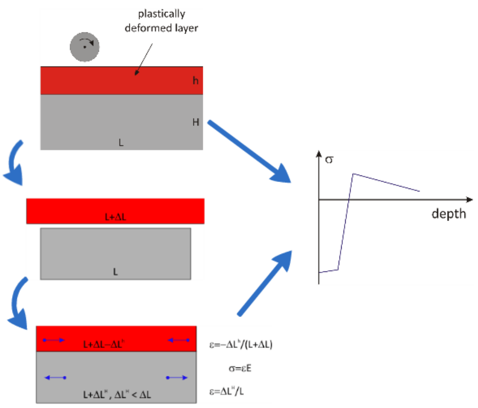

Mechanical

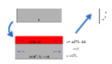

Thermal

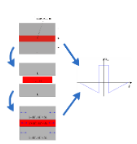

Metallurgical

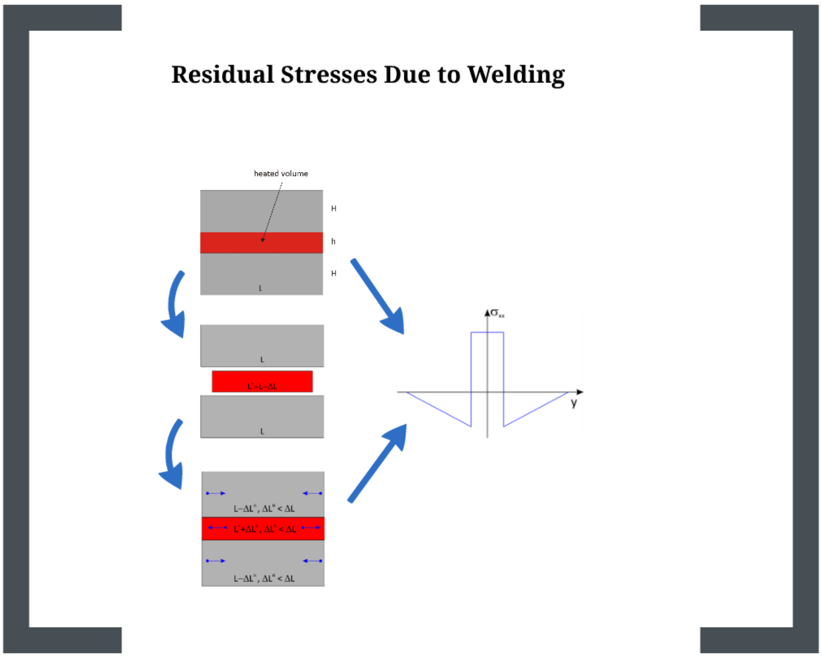
Residual Stresses Due to Welding
heated volume
H
h
H
L
L
L
y

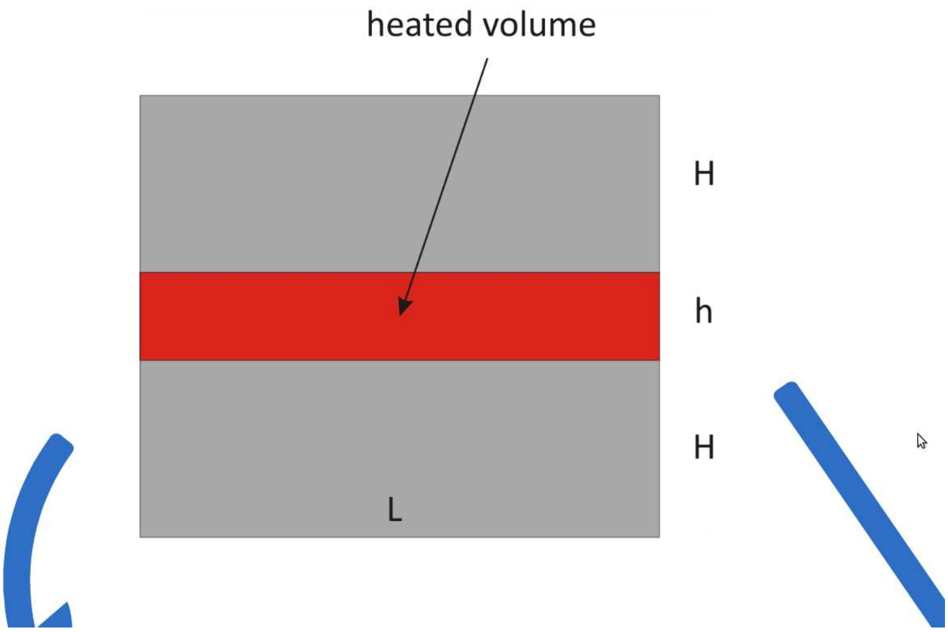
heated volume
H
h
H
L

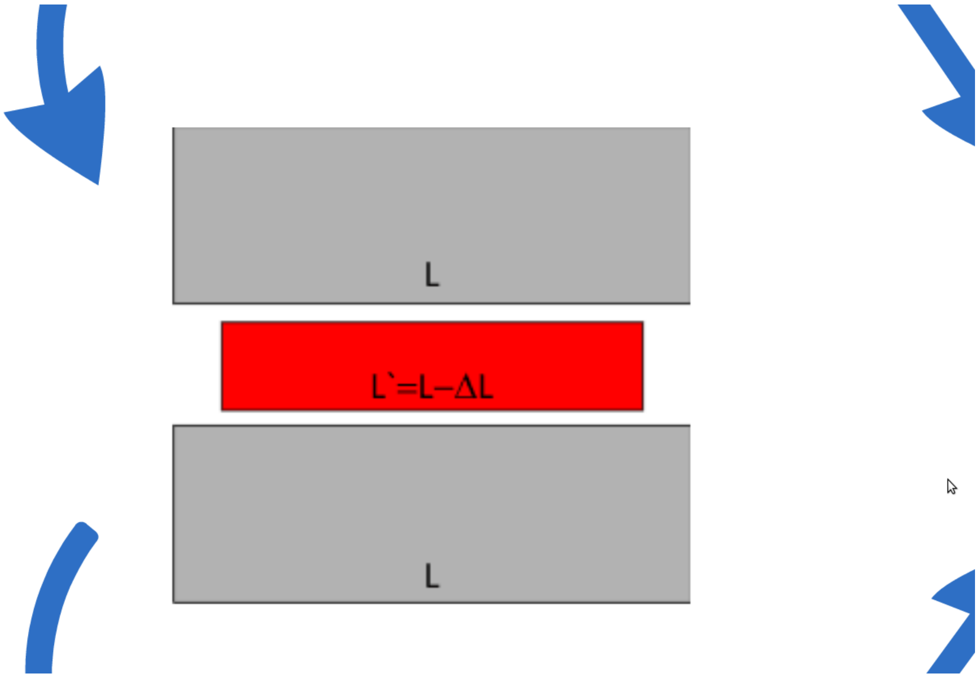
L
L`=L−ΔL
L

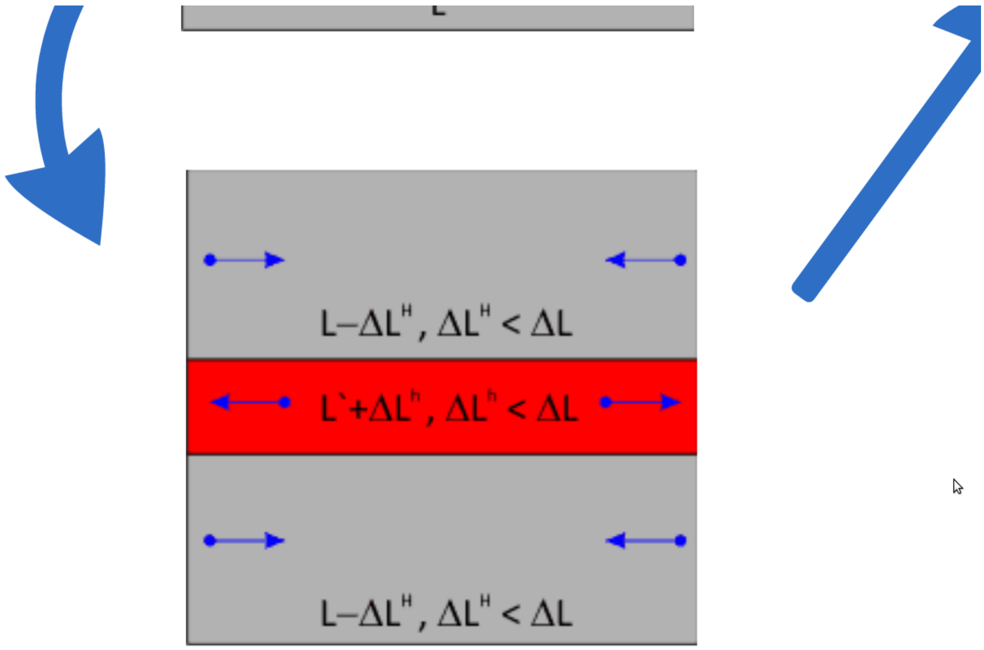
L−ΔL^H, ΔL^H < ΔL
L`+ΔL^h, ΔL^h < ΔL
L−ΔL^H, ΔL^H < ΔL

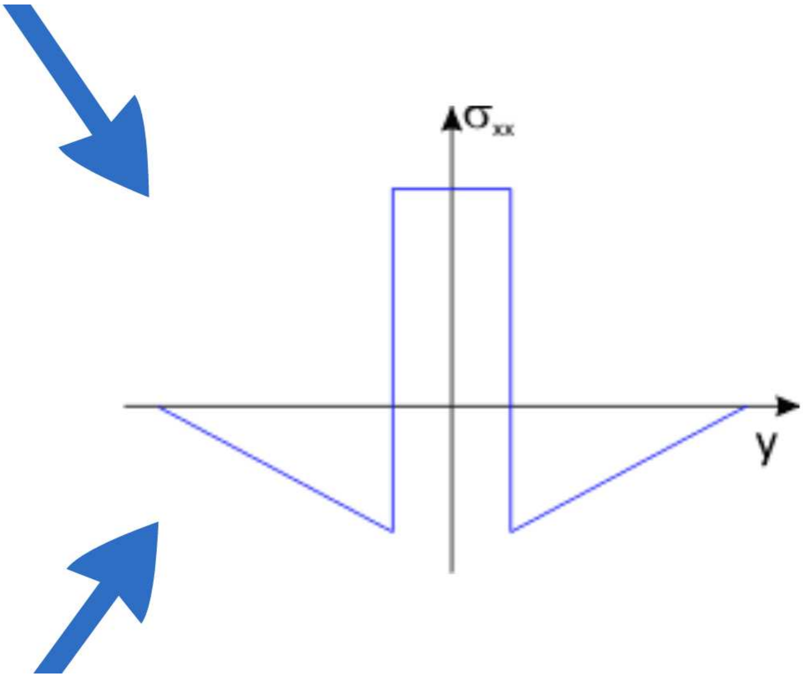
σxx
y

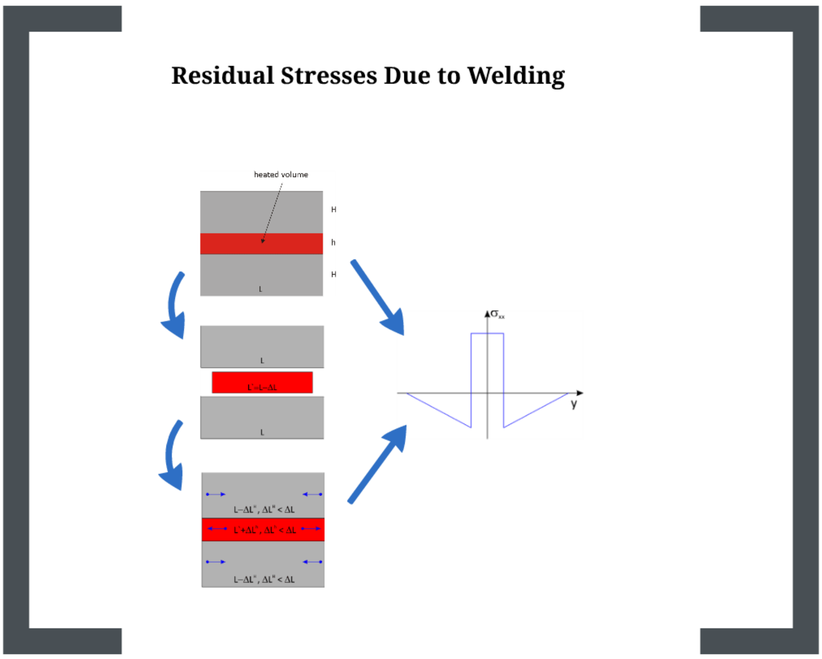
Residual Stresses Due to Welding
heated volume

Formation of residual stresses

Mechanical 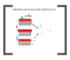

Thermal 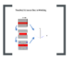

Metallurgical (Phase transformations with volume changes etc.)

Chemical (Carburizing and nitriding are similar to induction hardening, except the surface compressive residual stresses and case depth are not as deep.)

Effect of Residual Stresses

1. Distortion
2. Low cycle and high cycle fatigue performance
3. Stress corrosion cracking (SCC) and hydrogen initiated cracking (HIC)
4. Reduce buckling strength
5. Crack initiation and propagation. (Damage tolerance)

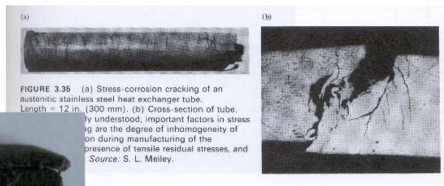

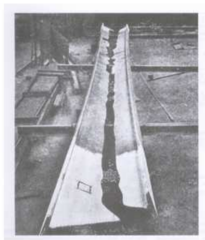

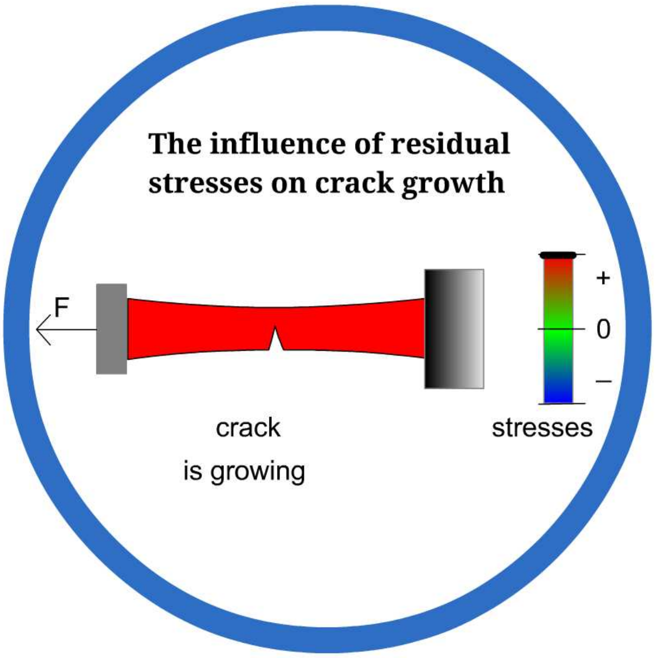
The influence of residual stresses on crack growth
F
+
0
–
crack
is growing
stresses

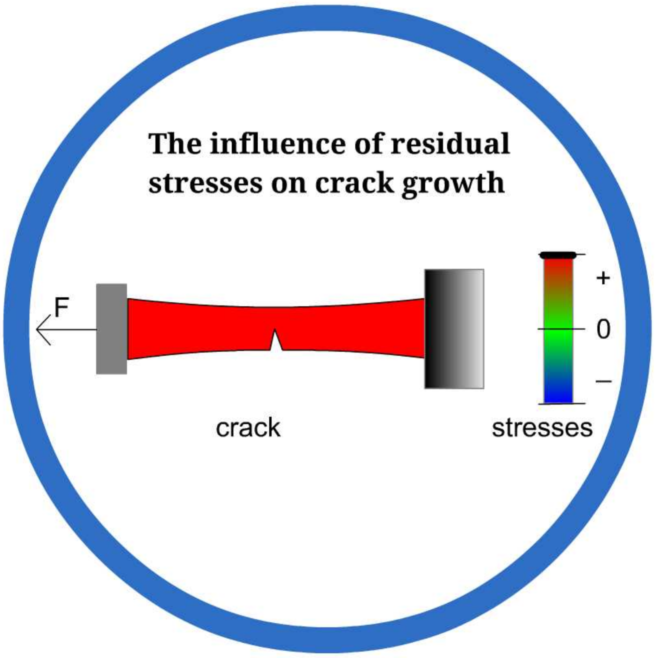
The influence of residual stresses on crack growth
F
+
0
–
crack
stresses

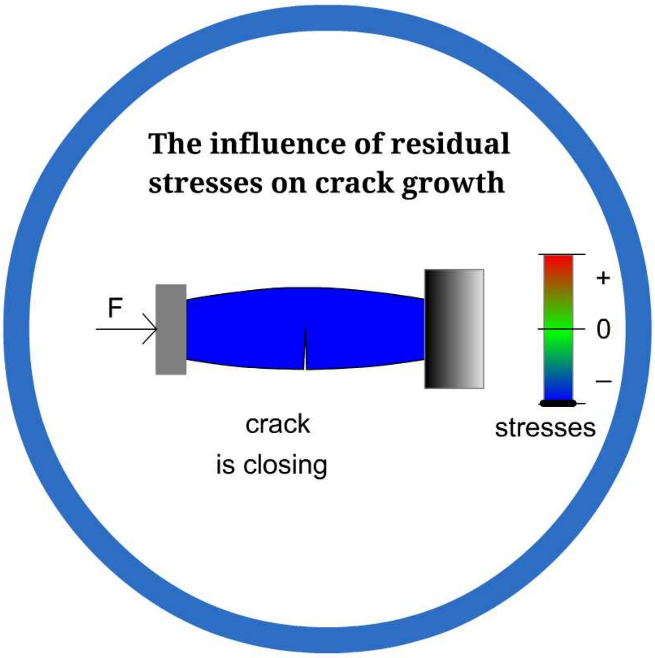
The influence of residual stresses on crack growth
F
+
0
–
crack
is closing
stresses

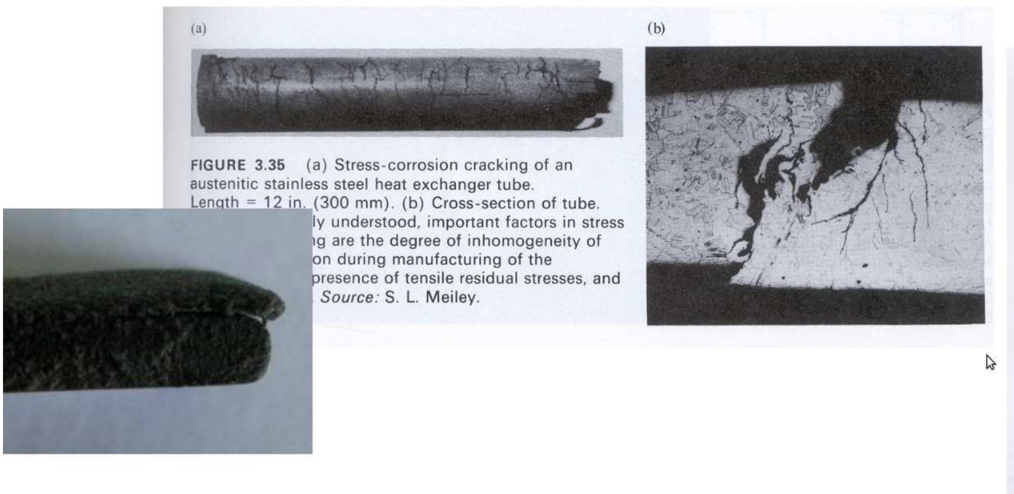
(a)
(b)
FIGURE 3.35 (a) Stress-corrosion cracking of an
austenitic stainless steel heat exchanger tube.
Length = 12 in. (300 mm). (b) Cross-section of tube.
ly understood, important factors in stress
g are the degree of inhomogeneity of
on during manufacturing of the
presence of tensile residual stresses, and
Source: S. L. Meiley.

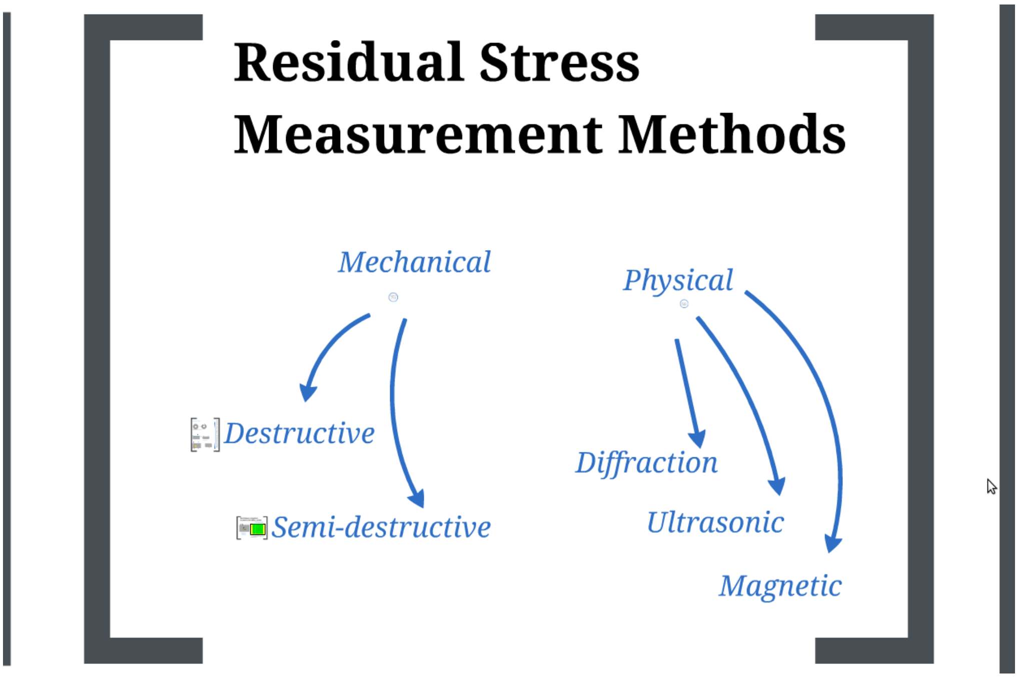
Residual Stress
Measurement Methods
Mechanical
Physical
Destructive
Semi-destructive
Diffraction
Ultrasonic
Magnetic

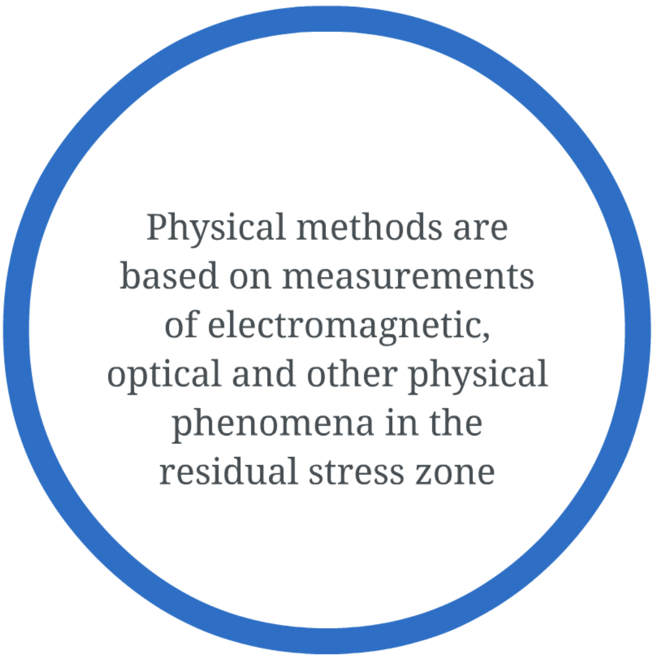
Physical methods are based on measurements of electromagnetic, optical and other physical phenomena in the residual stress zone

Mechanical techniques are called Stress-relaxation methods, which analyze the stress-relaxation produced in a metal part when material is removed. By measuring the deformation caused by the relaxation, the values of the residual stresses present in the part before the metal was removed can be determined by analyzing the successive state of equilibrium

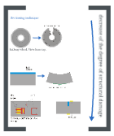

Destructive

Semi-destru

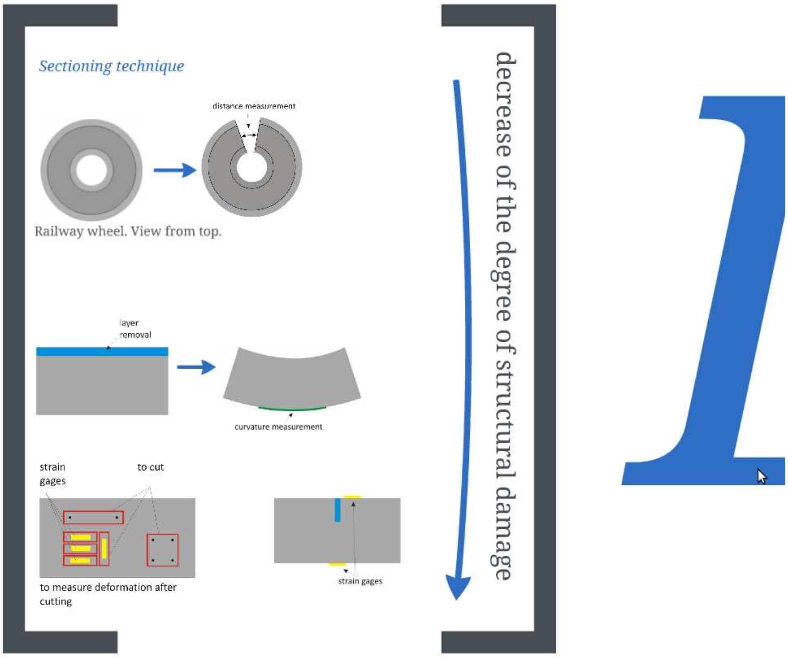

Sectioning technique

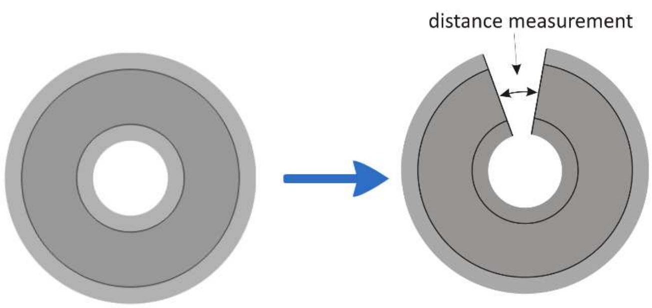

Railway wheel. View from top.

Railway wheel. View from top.

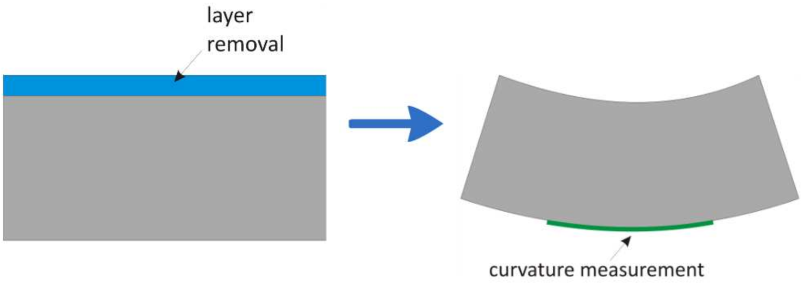

strain
gages

to cut

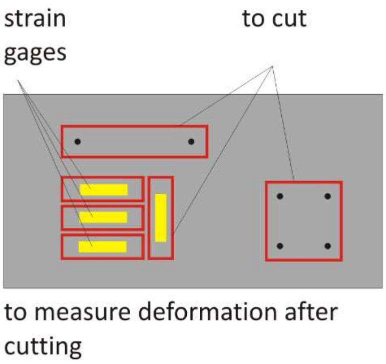

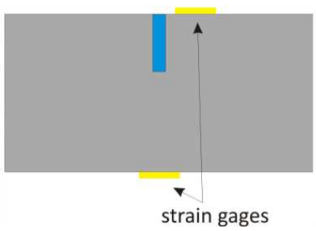

Destructive

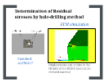

Semi-destructive

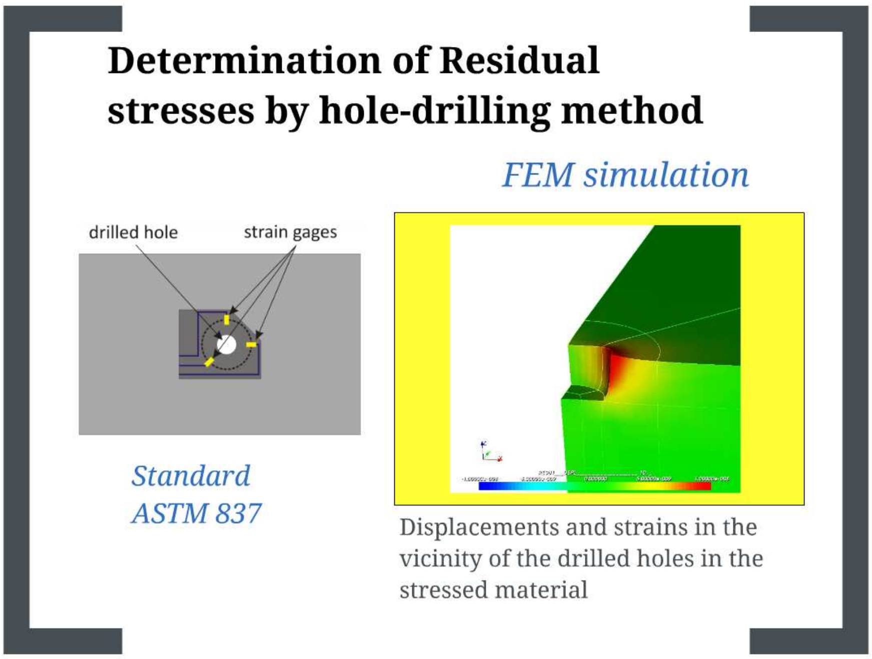

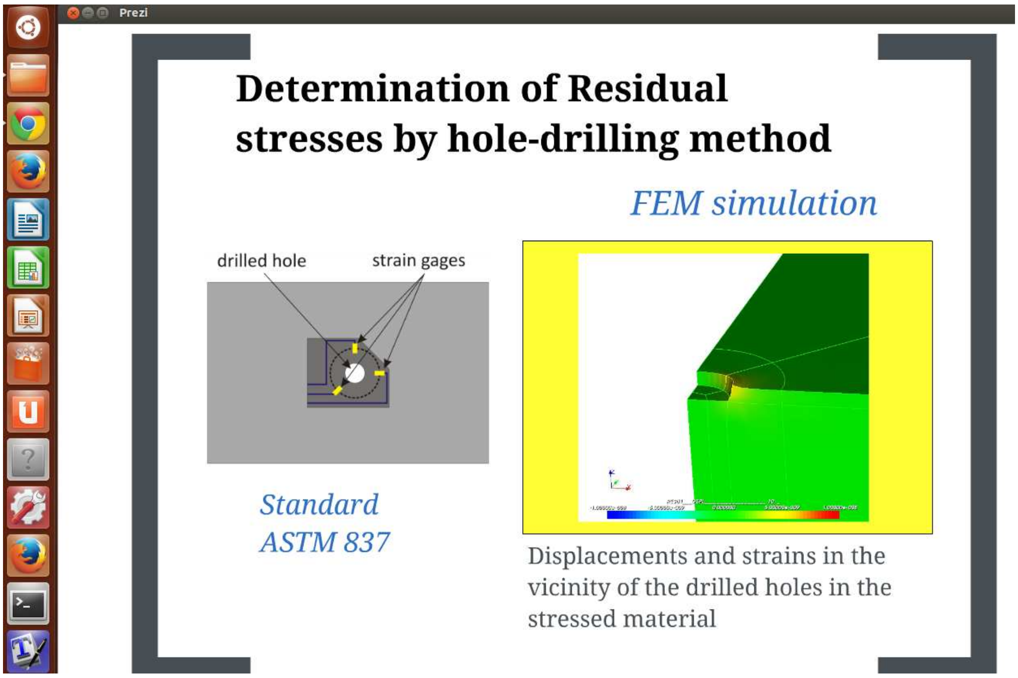
Prezi
Determination of Residual stresses by hole-drilling method
FEM simulation
drilled hole
strain gages
Standard ASTM 837
Displacements and strains in the vicinity of the drilled holes in the stressed material

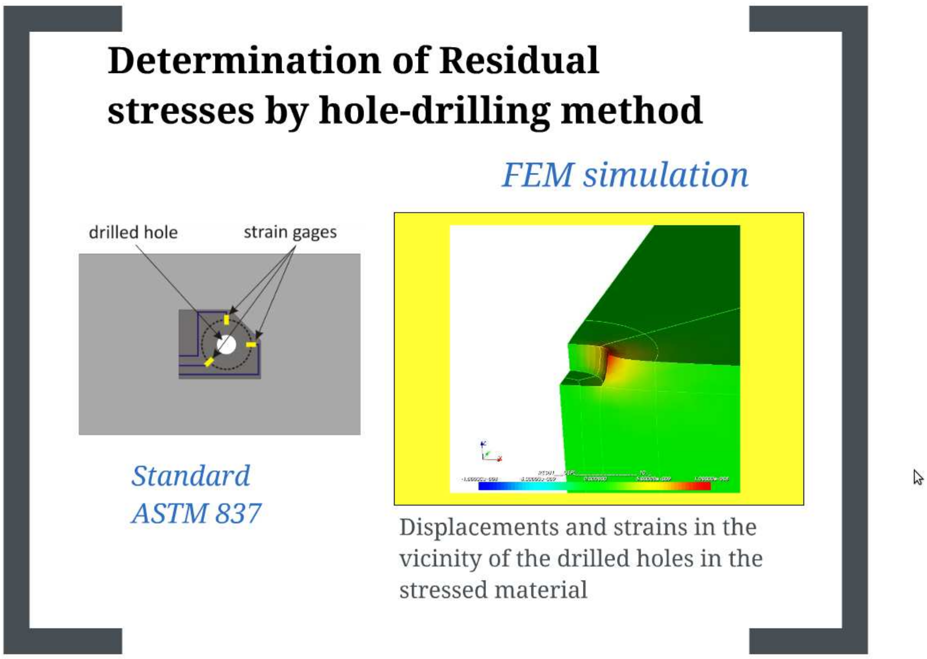
Determination of Residual stresses by hole-drilling method
FEM simulation
drilled hole
strain gages
Standard ASTM 837
Displacements and strains in the vicinity of the drilled holes in the stressed material

Speckle-interferometry

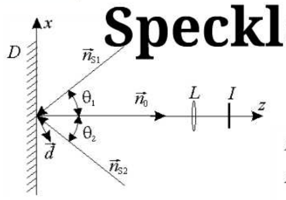

The optical scheme of a speckle-interferometer:
D - surface of the object,
I - image plane

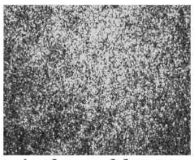

A typical speckle pattern formed by coherent illumination of a diffuse surface

$$I_1 = J_1 + J_2 + 2\sqrt{J_1 J_2}\cos(\Psi) \qquad (1)$$

$$I_2 = J_1 + J_2 + 2\sqrt{J_1 J_2}\cos\left(\Psi + \Delta\varphi(\vec{d})\right) \qquad (2)$$

$$\rho(\Delta\varphi_c) = \frac{\langle I_1 I_2\rangle - \langle I_1\rangle\langle I_2\rangle}{\sigma_{J_1}\sigma_{J_2}} \qquad \sigma_{J_2} = \sqrt{\langle I_2{}^2\rangle - \langle I_2\rangle^2} \quad \sigma_{J_1} = \sqrt{\langle I_1{}^2\rangle - \langle I_1\rangle^2} \qquad (3)$$

$$\rho_{J_1 J_2} = \frac{1 + \cos\left(\Delta\varphi(\vec{d})\right)}{2} \qquad (4)$$

$$I = a + b\cos(\Delta\varphi) \qquad (5)$$

$$\Delta\varphi(\vec{d}) = \frac{2\pi(\vec{n}_0 - \vec{n}_{S1})\cdot\vec{d}}{\lambda} - \frac{2\pi(\vec{n}_0 - \vec{n}_{S2})\cdot\vec{d}}{\lambda} = \frac{2\pi(\vec{n}_{S2} - \vec{n}_{S1})\cdot\vec{d}}{\lambda} \qquad (6)$$

$$\vec{n}_{S2} - \vec{n}_{S1} = (\sin\theta_1, 0, \cos\theta_1)^T - (-\sin\theta_1, 0, \cos\theta_1)^T = 2\sin\theta_1(1,0,0)^T \qquad (7)$$

$$\Delta\varphi(\vec{d}) = \frac{2\pi(\vec{n}_{S2} - \vec{n}_{S1})\cdot\vec{d}}{\lambda} = \frac{4\pi\sin\theta_1(1,0,0)\cdot(d_x, d_y, d_z)^T}{\lambda} = \frac{4\pi d_x\sin\theta_1}{\lambda} \qquad (8)$$

$$d_x = \frac{\lambda}{4\pi\sin\theta_1}\Delta\varphi(\vec{d}) \qquad (9)$$

Displacement measuring using ESPI-method

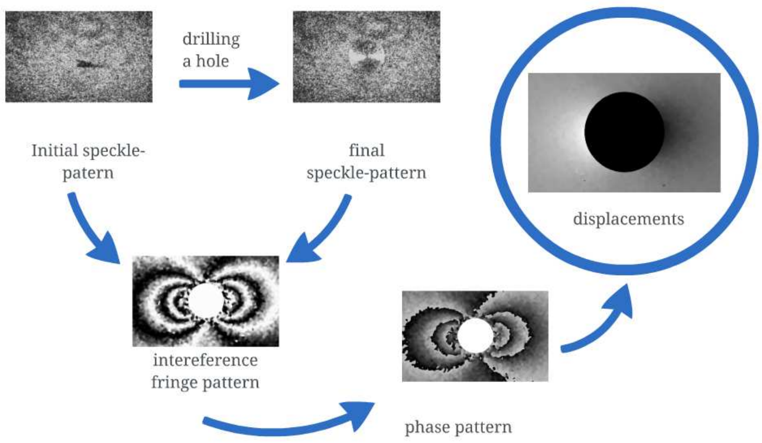

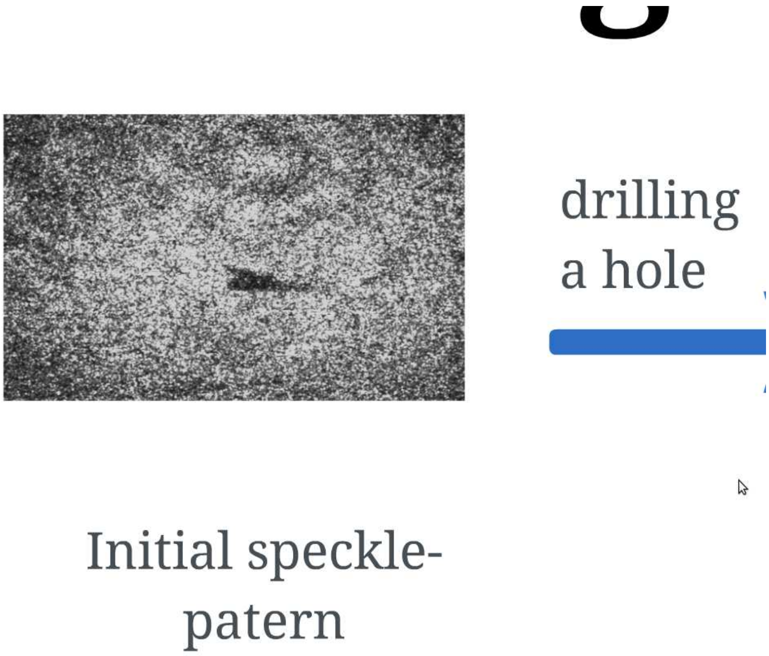
drilling
a hole
Initial speckle-
patern

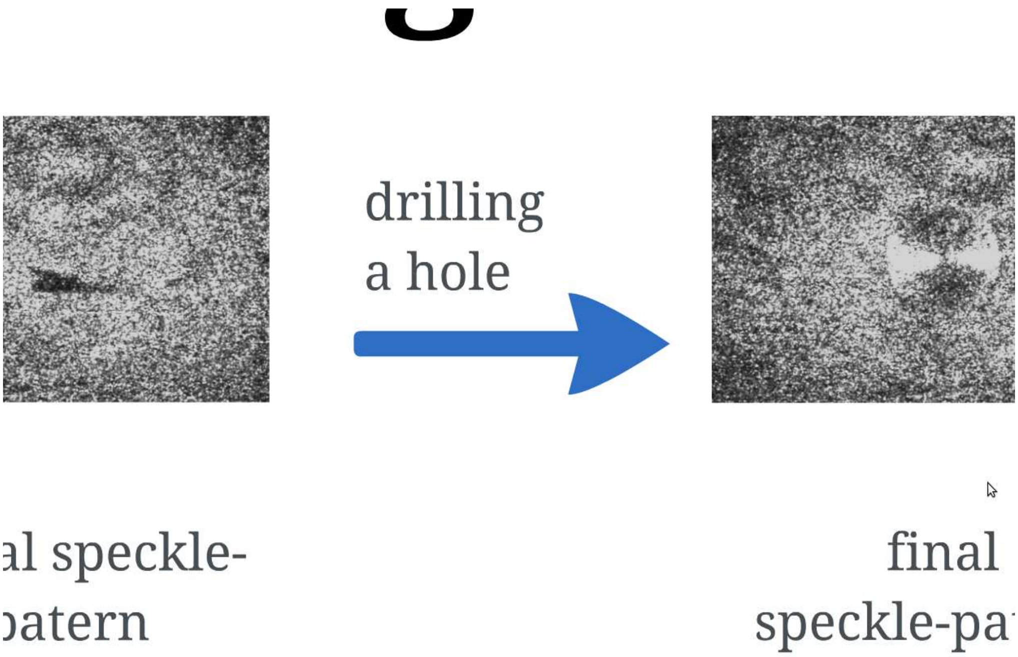
drilling
a hole
final

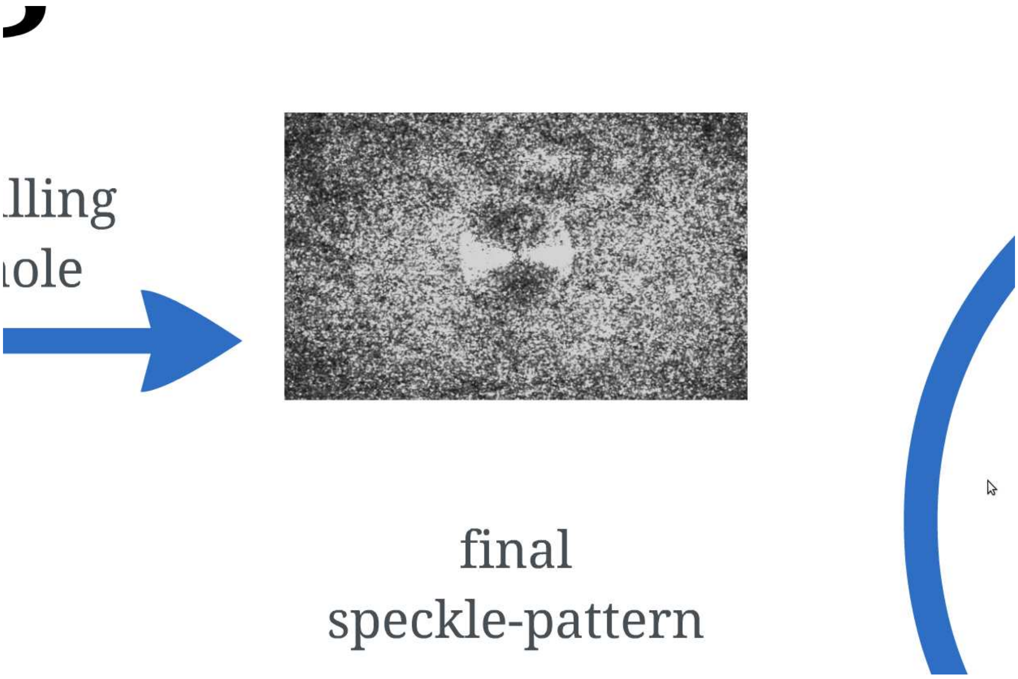
final
speckle-pattern

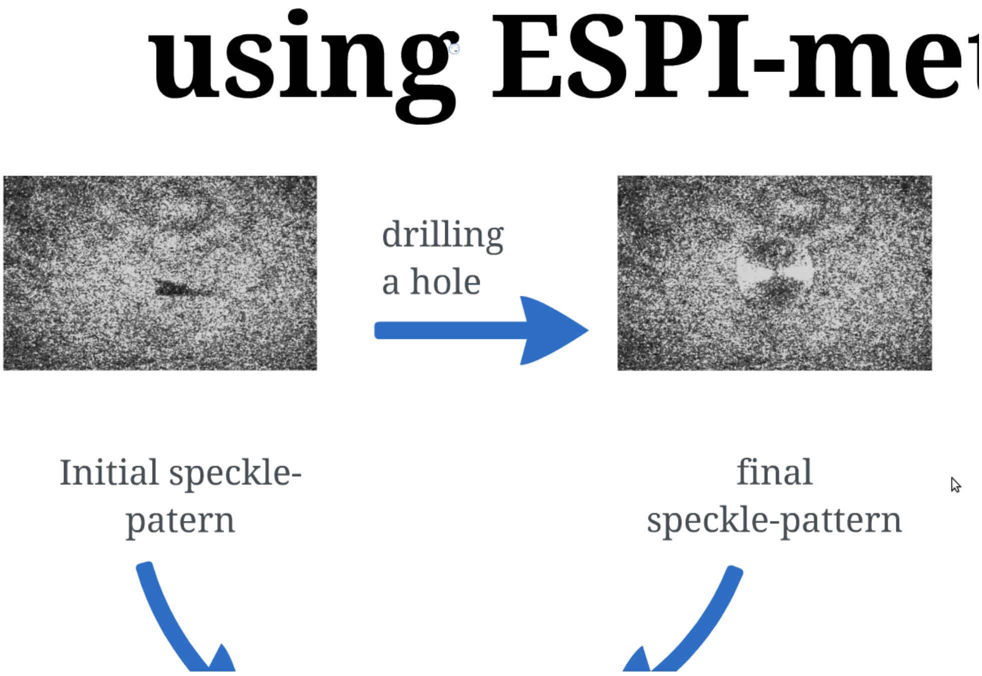
using ESPI-me
drilling
a hole
Initial speckle-
patern
final
speckle-pattern

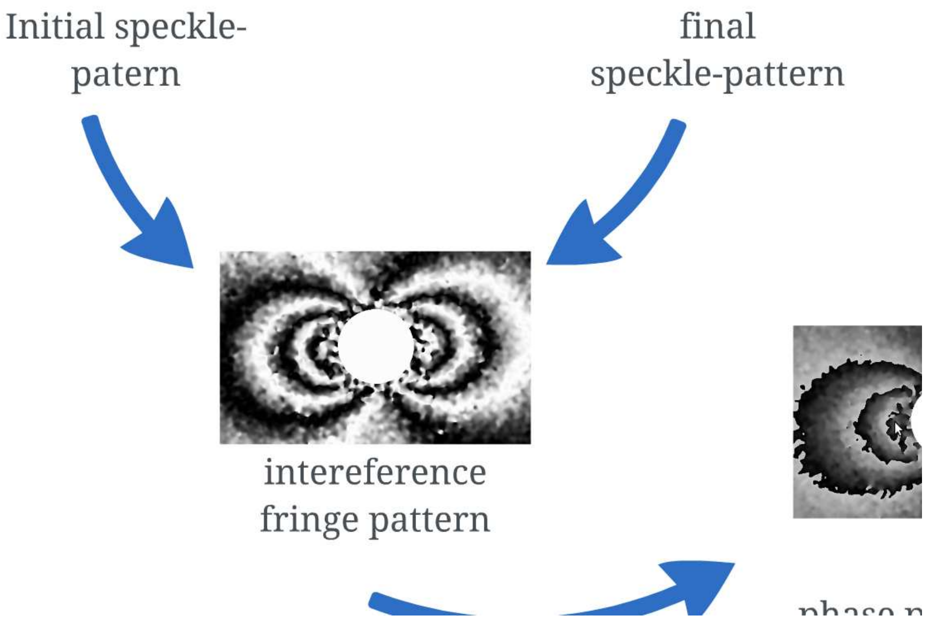
Initial speckle-
patern
final
speckle-pattern
intereference
fringe pattern

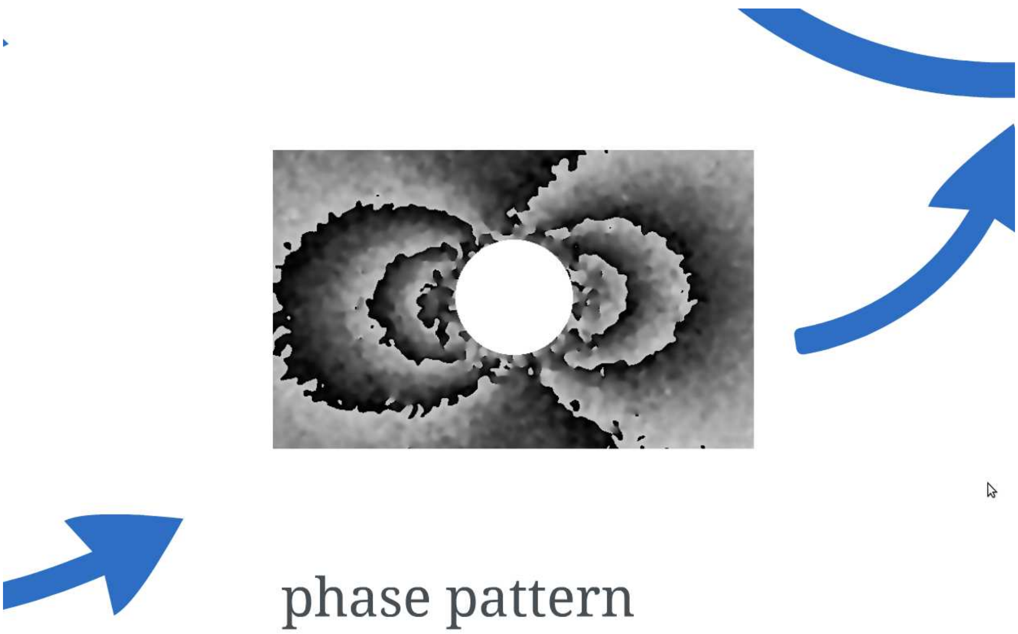
phase pattern

Displacement measuring using ESPI-method

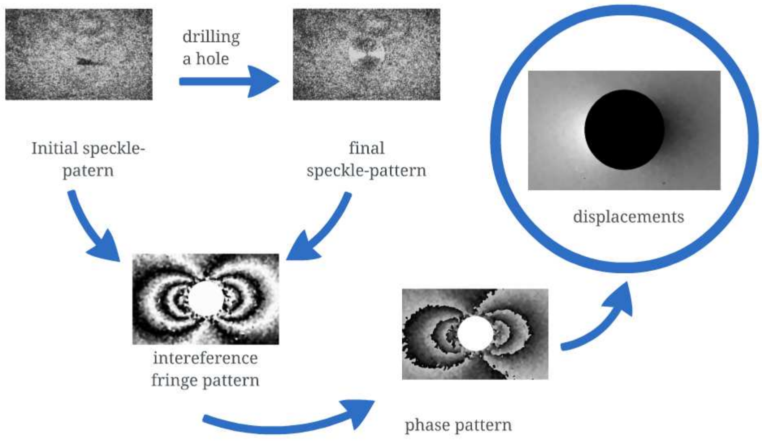

Residual stresses calculation using displacements data around a hole

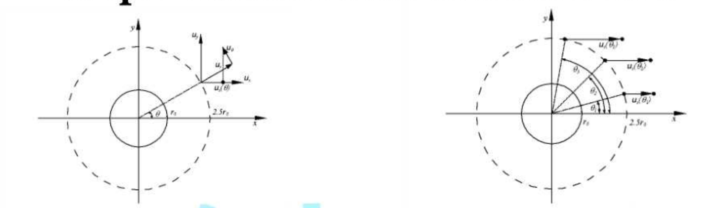

$$u_r(r,\theta) = \overline{A}(\sigma_{xx} + \sigma_{yy}) + \overline{B}[(\sigma_{xx} - \sigma_{yy})\cos 2\theta + 2\tau_{xy}\sin 2\theta] \quad (1)$$

$$u_\theta(r,\theta) = \overline{C}[(\sigma_{xx} - \sigma_{yy})\sin 2\theta - 2\tau_{xy}\cos 2\theta] \quad (2)$$

$$u_x(r,\theta) = u_r(r,\theta)\cos\theta - u_\theta(r,\theta)\sin\theta \quad (3)$$

$$u_x(\theta)\big|_{r=2.5r_0} = F(\theta)\sigma_{xx} + G(\theta)\sigma_{yy} + H(\theta)\tau_{xy} \quad (4)$$

$$\begin{bmatrix} F(\theta_1) & G(\theta_1) & H(\theta_1) \\ F(\theta_2) & G(\theta_2) & H(\theta_2) \\ F(\theta_3) & G(\theta_3) & H(\theta_3) \end{bmatrix} \begin{Bmatrix} \sigma_{xx} \\ \sigma_{yy} \\ \tau_{xy} \end{Bmatrix} = \begin{Bmatrix} u_x(\theta_1) \\ u_x(\theta_2) \\ u_x(\theta_3) \end{Bmatrix} \quad (5)$$

Determination of coefficients A, B и C

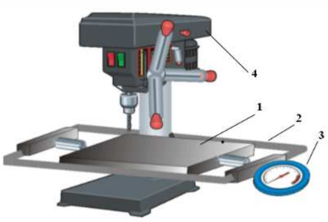

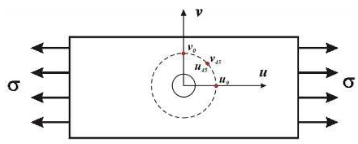

$$\overline{A} = \frac{u_0 + v_0}{2\sigma} = \frac{u_{45} + v_{45}}{\sqrt{2}\sigma} \quad (1)$$

$$\overline{B} = \frac{u_0 - v_0}{2\sigma} \quad (2)$$

$$\overline{C} = \frac{u_{45} - v_{45}}{\sqrt{2}\sigma} \quad (3)$$

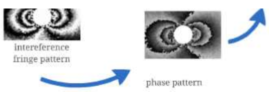

$$u_x(\theta)\big|_{r=2.5r_0} = F(\theta)\sigma_{xx} + G(\theta)\sigma_{yy} + H(\theta)\tau_{xy} \quad (4)$$

$$\begin{bmatrix} F(\theta_1) & G(\theta_1) & H(\theta_1) \\ F(\theta_2) & G(\theta_2) & H(\theta_2) \\ F(\theta_3) & G(\theta_3) & H(\theta_3) \end{bmatrix} \begin{Bmatrix} \sigma_{xx} \\ \sigma_{yy} \\ \tau_{xy} \end{Bmatrix} = \begin{Bmatrix} u_1(\theta_1) \\ u_2(\theta_2) \\ u_3(\theta_3) \end{Bmatrix} \quad (5)$$

Determination of residual stresses using speckle-interferometry method

Equipment for determination of RS

1 - speckle-interferometer; 2 - fiber; 3 - drilling device; 4 - laser; 5 - notebook

Software for determination of RS

User interface of the 'Fringe Viewer' software for ESPI-device controlling and preliminary image processing.

User interface of the 'Fringe Editor' software for calculation of residual stresses

Evaluation of the accuracy of the displacement measurements and RS determination

Problem about the bending of a console beam with a fixed end by a force applied to a free end

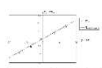

Comparison of theoretical and experimental determination of residual stresses

Determination of residual stresses in a railway wheel using ESPI-HD method

Equipment for determination of RS

1 - speckle-interferometer; 2 - fiber;
3 - drilling device; 4 - laser; 5 - notebook

Software for determination of RS

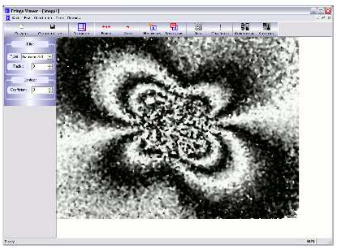

User interface of the 'Fringe Viewer' software for ESPI-device controlling and preliminary image processing.

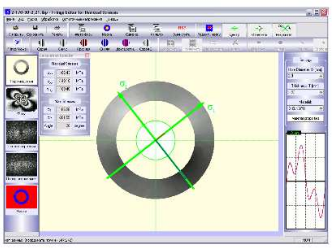

User interface of the 'Fringe Editor' software for calculation of residual stresses

Evaluation of the accuracy of the displacement measurements and RS determination

Problem about the bending of a console beam with a fixed end by a force applied to a free end

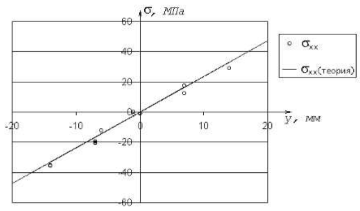

Comparison of theoretical and experimental determination of residual stresses

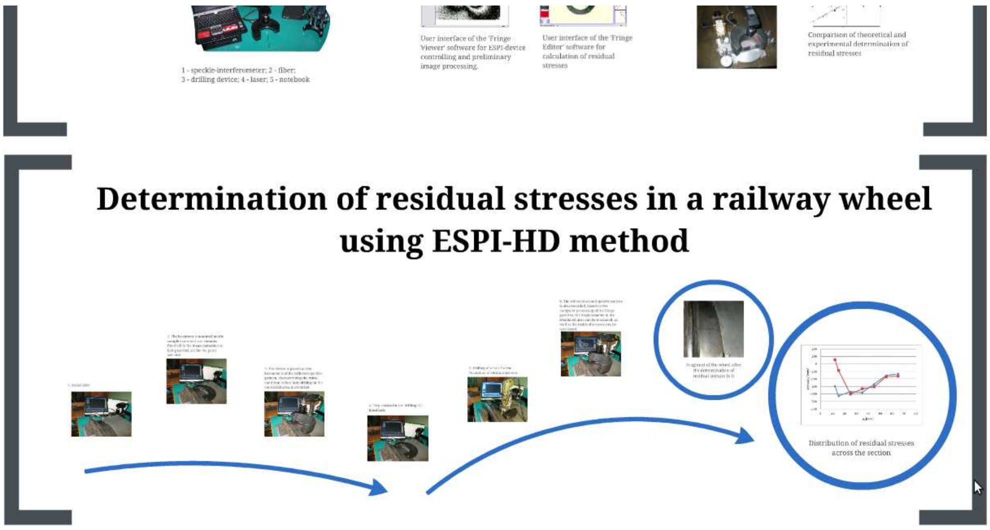

1. Initial state

2. The basement is mounted on the sample examined and remains fixed while the measurements are being carried out for the point selected.

3. The device is placed on the basement and the reflected speckle-pattern, characterizing the initial condition before hole-drilling in the controlled area, is recorded

4. Preparation for the drilling of a blind hole

5. Drilling of a hole for the relaxation of residual stresses

6. The reflected second speckle-pattern is also recorded. Based on the computer processing of the fringe patterns, the displacements in the irradiated area can be evaluated, as well as the residual stresses can be calculated.

Fragment of the wheel after
the determination of
residual stresses in it

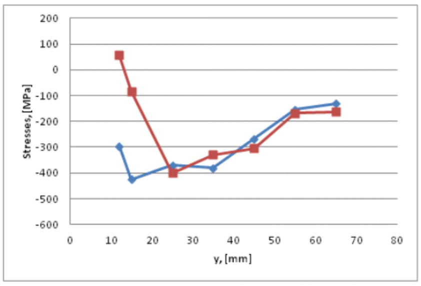

Distribution of residual stresses
across the section

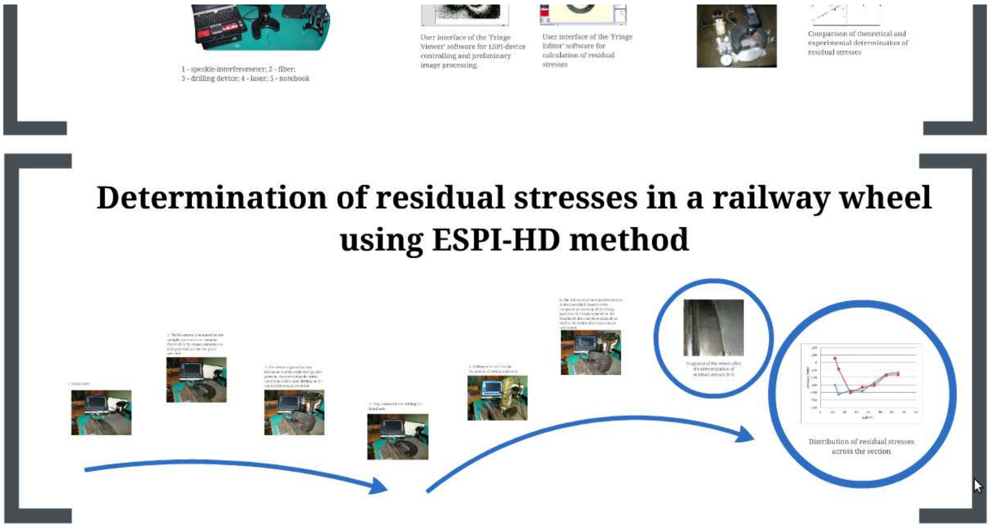

1 - speckle-interferometer; 2 - fiber; 3 - drilling device; 4 - laser; 5 - notebook
User interface of the 'Fringe Viewer' software for ESPI-device controlling and preliminary image processing
User interface of the 'Fringe Editor' software for calculation of residual stresses
Comparison of theoretical and experimental determination of residual stresses
Determination of residual stresses in a railway wheel using ESPI-HD method
Distribution of residual stresses across the section

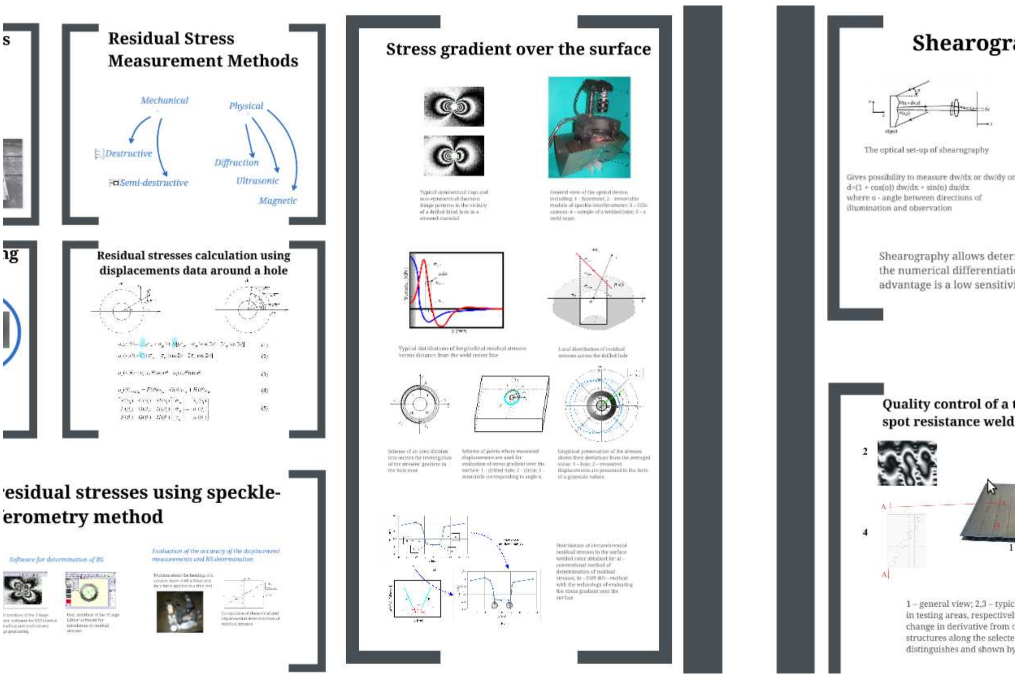

Residual Stress Measurement Methods
Mechanical
Physical
Destructive
Semi-destructive
Diffraction
Ultrasonic
Magnetic
Residual stresses calculation using displacements data around a hole
esidual stresses using speckle-
erometry method
Stress gradient over the surface
Shearogr
The optical set-up of shearography
Quality control of a
spot resistance weld

Stress gradient over the surface

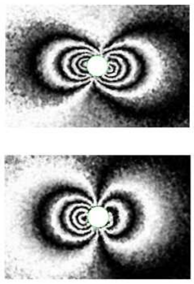

Typical symmetrical (top) and non-symmetrical (bottom) fringe patterns in the vicinity of a drilled blind hole in a stressed material

General view of the optical device, including: 1 – basement; 2 – removable module of speckle-interferometer; 3 – CCD-camera; 4 – sample of a welded joint; 5 – a weld seam.

stressed material

weld seam.

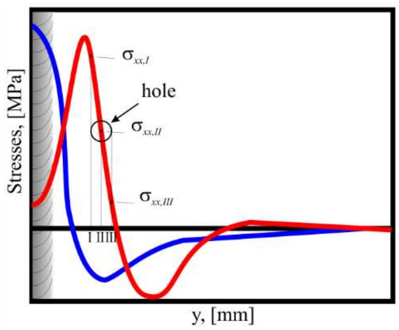

Typical distributions of longitudinal residual stresses versus distance from the weld center line.

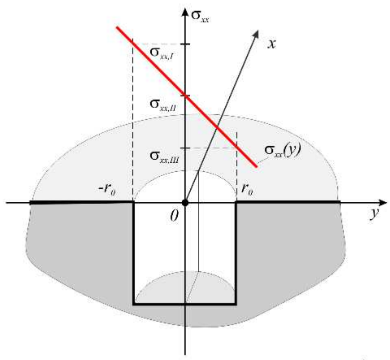

Local distribution of residual stresses across the drilled hole

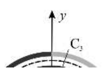

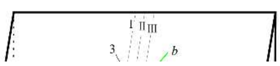

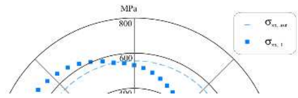

Typical distributions of longitudinal residual stresses versus distance from the weld center line.

Local distribution of residual stresses across the drilled hole

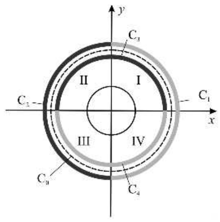

Scheme of an area division into sectors for investigation of the stresses' gradient in the hole zone

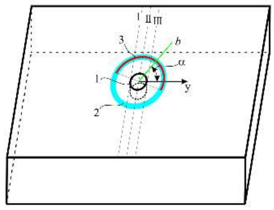

Scheme of points where measured displacements are used for evaluation of stress gradient over the surface: 1 – drilled hole; 2 – circle; 3 – semicircle corresponding to angle α.

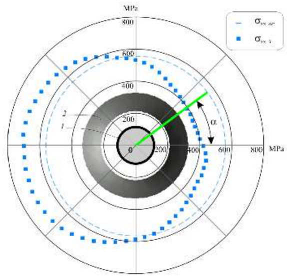

Graphical presentation of the stresses shows their deviations from the averaged value: 1 – hole; 2 – measured displacements are presented in the form of a grayscale values.

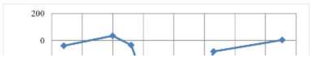

semicircle corresponding to angle α.

of a grayscale values.

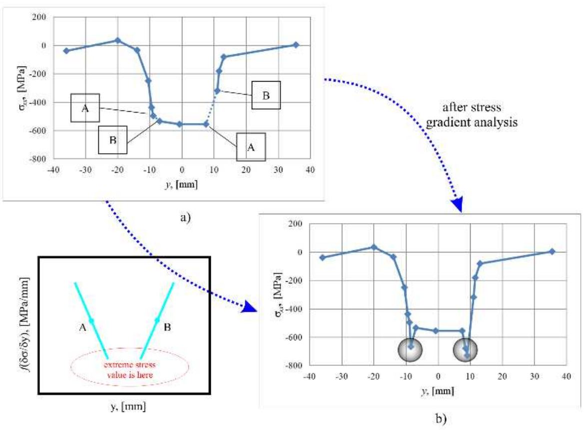

Distribution of circumferential residual stresses in the surface welded rotor obtained by: a) – conventional method of determination of residual stresses; b) – ESPI-HD – method with the technology of evaluating the stress gradient over the surface

The use of the ESPI-HD method makes it possible to increase the accuracy of residual stress determination and also gives an additional opportunity of the stress gradient assessment on the basis of the drilled out hole. The high sensitivity of the device enables to conduct the investigations of the stressed state on a small base (from 0.5 mm) without any loss of the experiment accuracy. The procedure of residual stress determination, compactness of the equipment and efficiency of the computer processing of the optical information open the new possibilities for examining the structures under the laboratory and industrial conditions.

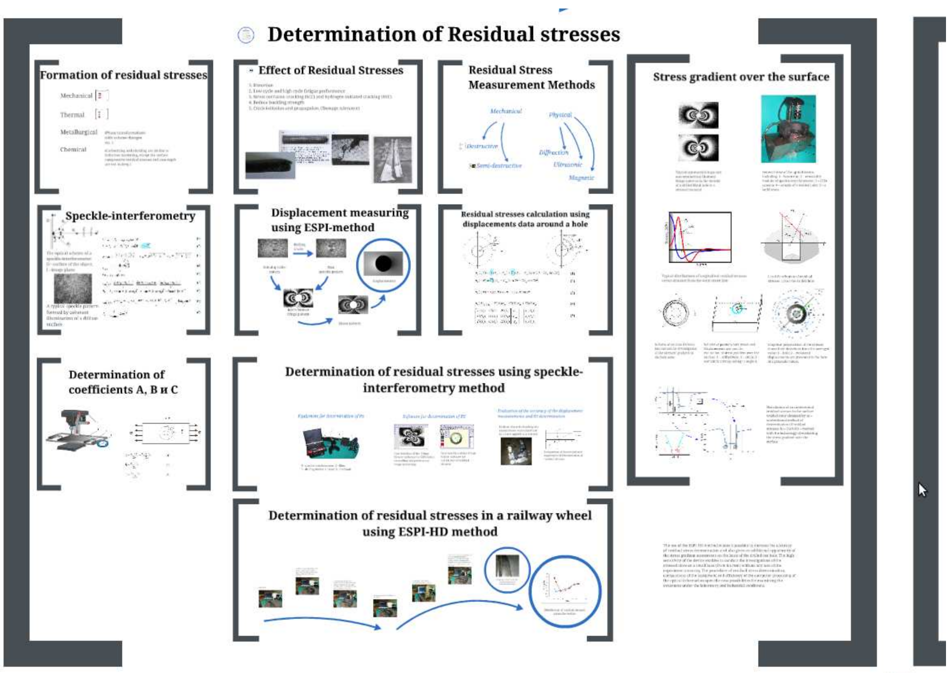

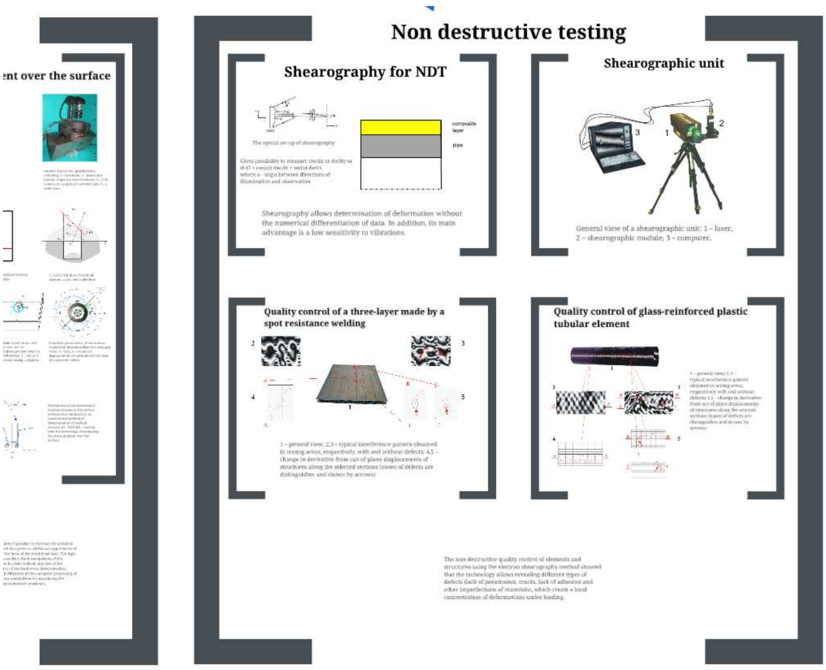

Shearography for NDT

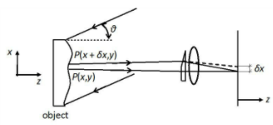

The optical set-up of shearography

Gives possibility to measure dw/dx or dw/dy or
d=(1 + cos(o)) dw/dx + sin(o) du/dx
where o - angle between directions of
illumination and observation

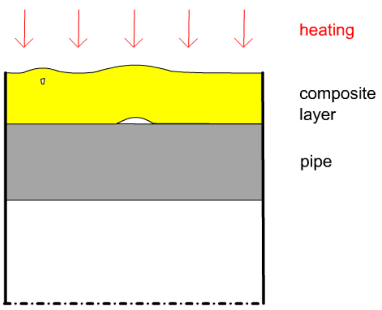

Shearography allows determination of deformation without the numerical differentiation of data. In addition, its main advantage is a low sensitivity to vibrations.

Shearography for NDT

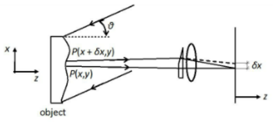

The optical set-up of shearography

Gives possibility to measure dw/dx or dw/dy or d=(1 + cos(o)) dw/dx + sin(o) du/dx
where o - angle between directions of illumination and observation

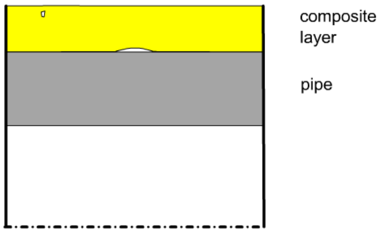

Shearography allows determination of deformation without the numerical differentiation of data. In addition, its main advantage is a low sensitivity to vibrations.

Shearographic unit

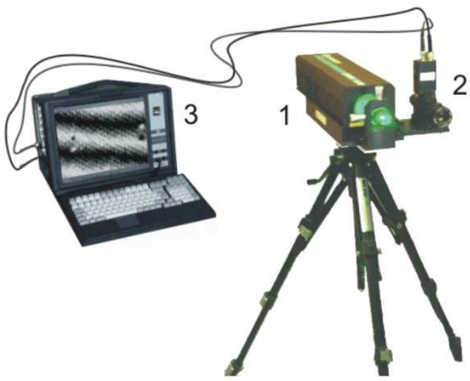

General view of a shearographic unit: 1 – laser, 2 – shearographic module; 3 – computer.

Quality control of a three-layer made by a spot resistance welding

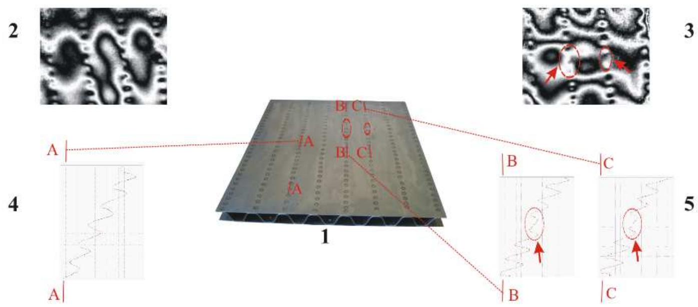

1 – general view; 2,3 – typical interference pattern obtained in testing areas, respectively, with and without defects; 4,5 – change in derivative from out-of-plane displacements of structures along the selected sections (zones of defects are distinguishes and shown by arrows)

Quality control of glass-reinforced plastic tubular element

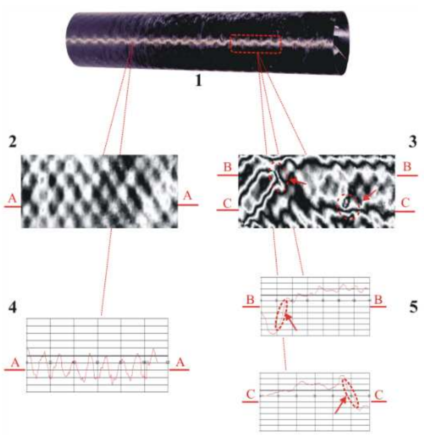

1 – general view; 2,3 – typical interference pattern obtained in testing areas, respectively, with and without defects; 4,5 – change in derivative from out-of-plane displacements of structures along the selected sections (zones of defects are distinguishes and shown by arrows)

The non-destructive quality control of elements and structures using the electron shearography method showed that the technology allows revealing different types of defects (lack of penetration, cracks, lack of adhesion and other imperfections of materials), which create a local concentration of deformations under loading.

The above-mentioned contactless optical methods, compact devices and instruments make it possible to perform the nondestructive quality control and determination of stressed state of elements and structures made from metallic and composite materials. The application of ESPI and shearography methods opens up new opportunities for the nondestructive diagnostics of structures under the conditions of their manufacture and service.